Supporting info for: "Directing SEI formation on Si-based electrodes using atomic layer deposition"

Supti Das,[a] Anders Brennhagen,[a] Carmen Cavallo,[a‡] Veronica Anne-Line Kathrine Killi,[a] Ingvild Thue Jensen,[b] Annett Thøgersen,[b] Jan Petter Mæhlen,[c] Samson Yuxiu Lai,[c] Ola Nilsen[a] and Alexey Y. Koposov[a, c]*

a. Centre for Materials Science and Nanotechnology, Department of Chemistry, University of Oslo, PO Box 1033, Blindern, 0315, Oslo, Norway.
b. SINTEF Industry, Materials Physics, Forskningsveien 1, 0373 Oslo, Norway
c. Department of Battery Technology, Institute for Energy Technology (IFE), Instituttveien 18, 2007, Kjeller, Norway.
‡ Present address: FAAM, Strada Statale Via Appia 7 bis – 81030, Teverola (CE), Italy

1. Experimental

Atomic layer deposition (ALD) of TiO_2 on amorphous silicon particles

Pristine amorphous silicon nanoparticles with an average size of 40 nm were received from Cenate AS (nano40, H18-1) and stored in the glovebox under argon atmosphere. The samples were coated in a home-built atomic layer deposition (ALD) reactor optimized for coating into porous structures. The precursors used were titanium (IV) tetrachloride ($TiCl_4$) (≥ 99 % from MERCK) and distilled H_2O (resistivity > 1 MΩ·cm) as delivered by vapor draw from containers kept at room temperature. The deposition temperature was kept at 150 °C or 170 °C where stated. Where water pretreatment was used, as in a-Si-T4 and T5, a sequence of 50 cycles of 1 s pulse, 5 s hold and 100 s purge was used. The typical deposition sequence consisted of 2 s pulse time of $TiCl_4$, 5 s hold, 50 s purge and 1 s pulse time of H_2O, 5 s hold and 100 s purge. Both the hold and the purges contain pressure buildups and purges (from ca. 1 to 10 mbar) using N_2 to better distribute the reactants. The number of deposition cycles were 400 for all samples.

Table S1: Overview of sample IDs and experimental conditions for attempts of TiO_2 coating on amorphous silicon particles (a-Si) using ALD.

Sample ID	Pulse time		Deposition temperature (°C)	Water pretreatment	Other modifications
	$TiCl_4$	H_2O			
a-Si-T1	2 s	1 s	150	No	
a-Si-T2	2 s	1 s	150	No	Stored in air
a-Si-T3	20 s	10 s	150	No	

a-Si-T4	20 s	10 s	150	Yes	
a-Si-T5	20 s	10 s	170	Yes	

The changes to the standard ALD process were made to ensure saturation of active sites on the powder surface, and the extra water cycles were added to gently oxidize the surface of the silicon nanoparticles.

Materials characterization

The morphologies and microstructure of amorphous silicon (a-Si) and TiO_2-coated amorphous Si (a-Si-Tx, x = 1-5) prepared by ALD were studied by transmission electron microscopy (TEM). Detailed analysis of the TiO_2-coated a-Si powder was performed using scanning transmission electron microscopy (STEM) on a Thermo Fisher Scientific Titan G2 60-300 operated at 300 kV, with a Gatan GIF Quantum 965 electron energy loss spectroscopy (EELS) spectrometer and a Super-X energy dispersive X-ray spectroscopy (EDS) detector. For analysis, the powder was distributed dry on a holey carbon film supported by a Cu grid. The Cu grid was mounted to the sample holder in open atmosphere. In this process, the Si particles were exposed to air for ~5 min. EELS data analysis was conducted using Gatan Digital Micrograph software, and EDS analysis was performed using Thermo Fisher Scientific Velox software.

Electrode preparation

The electrodes were prepared using aqueous slurries containing active material powders (60 wt% a-Si or TiO_2-coated a-Si), sodium carboxymethyl cellulose binder (15 wt%, CMC, Sigma-Aldrich), graphite (10 wt%, TIMCAL KS6) and carbon black (15 wt%, TIMCAL Super C65). The binder was dissolved in aqueous solution (buffer solution of pH 2.87, made from KOH, citric acid and deionized water) and mixed using a centrifugal mixer (Thinky, Co., ARE-250CE). Then Si, graphite, carbon black and deionized water were added and mixed in the mixer again and the slurry was tape casted on double sided dendritic copper foil (99.9%, 10 μm thick, Schlenck) with doctor blade wet thickness of 200 μm. After drying overnight in open atmosphere, the electrodes were punched into discs of 15 mm in diameter and dried at 80 °C under dynamic vacuum in a Büchi oven for 12 h and kept inside the glovebox for cell assembly.

Electrochemical characterization

The electrochemical properties of the pristine and coated amorphous Si electrodes were investigated in CR2032 coin cells (MTI). The cells were assembled with Li foil (MTI, Li chips, diameter 15.6 mm, thickness 250 μm) as counter electrode, Si electrode as working electrode and Whatman glass fiber filter (17mm, GF/F) as separator in an argon-filled glove box (MBraun) with water and oxygen levels below 0.1 ppm. 70 μl of the liquid electrolyte consisting of 1.2 M $LiPF_6$ in 3:7 vol% ethylene carbonate:ethylmethyl carbonate (EC:EMC), respectively, 2 wt% of

vinylene carbonate (VC) as additive and both with/without 10 wt% of fluoroethylene carbonate (FEC, Solvonic) were used. The half cells were measured using multichannel battery tester (Neware, BTS) in the voltage range between 0.05–1.00 V vs Li/Li^+ with 3 formation cycles at C/20 followed by cycling at C/10.

Electrochemical impedance spectroscopy (EIS) measurements were performed at room temperature (25 °C) using Biologic MPG2 by applying an alternating current (AC) voltage amplitude of 10 mV over a frequency range of 20 mHz to 20 kHz.

Post-mortem X-ray photoelectron spectroscopy (XPS) and scanning electron microscopy (SEM)

Delithiated ex situ samples for XPS and SEM measurements were prepared by extracting the electrodes from coin cells disassembled with a disassembling tool (Hohsen) after cycling for 20 cycles at C/10 in addition to the 3 formation cycles at C/20 with FEC-free electrolyte (1.2 M $LiPF_6$ in EC:EMC (7:3 vol%) and 2 wt% VC). The electrodes were washed with DMC before being inertly transferred to the instruments.

Scanning electron microscopy (SEM), a Thermo Fisher Scientific Nova NanoSEM 650, using the concentric back-scattered (CBS) detector was used to get an overview of the cycled electrodes. The electrodes were cut with a JEOL IB-19520CCP cross section polisher using Ar ions at 6 kV and 3 kV.

X-ray photoelectron spectroscopy (XPS) was performed using a Thermo Theta Probe instrument with monochromatic Al Kα radiation (hν=1486.6 eV) operated at 15 kV and 15 mA and with a 400 µm diameter spot size. Survey spectra were collected at a pass energy (PE) of 200 eV with step size 1 eV, while high resolution spectra were collected at PE=40 eV with a step size of 0.1 eV. The XPS data were analyzed using the CasaXPS software[1] after Shirley background subtraction.[2] Due to differential sample charging, the binding energy (BE) scale was post-calibrated by aligning the C-O component in the C 1s spectra. This also gave fair alignment of F 1s, P 2p, Li 1s and the Si oxide region in Si 2p.

2. Supplementary figures and results

Transmission electron microscopy (TEM)

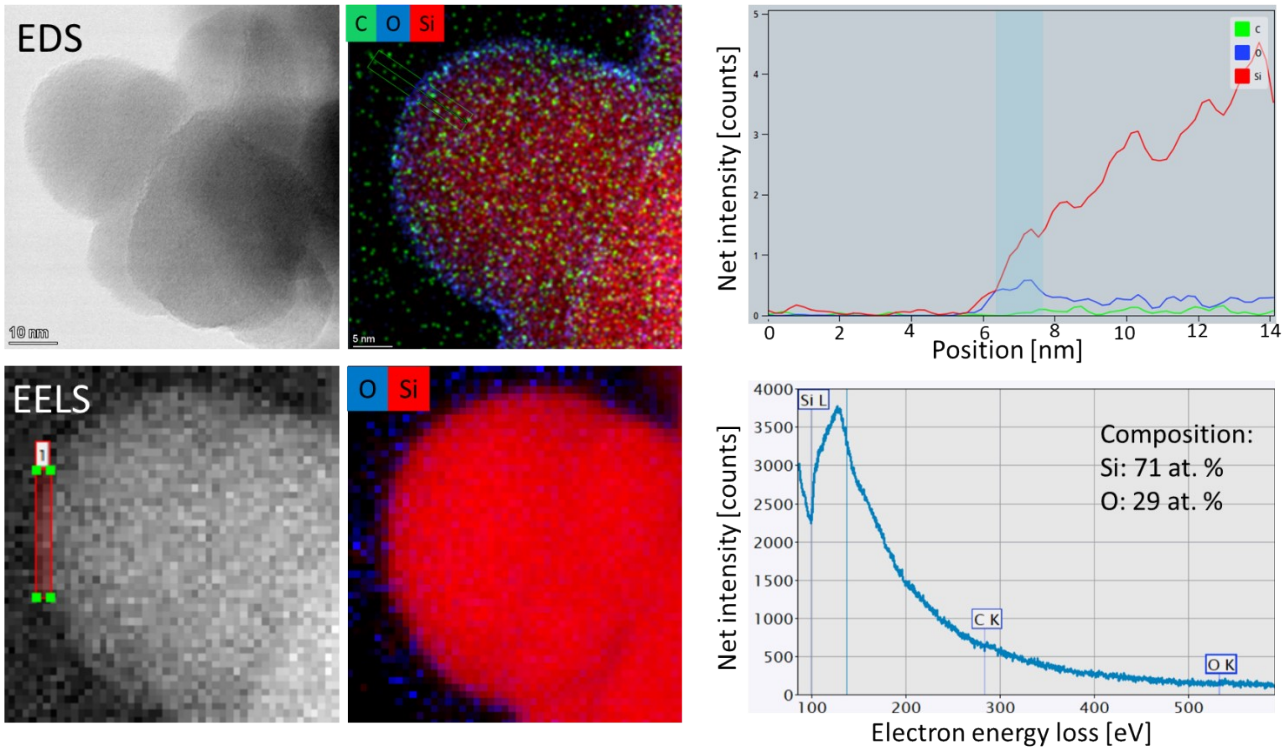

Fig. S1: EDS and EELS mapping and TEM images of uncoated a-Si.

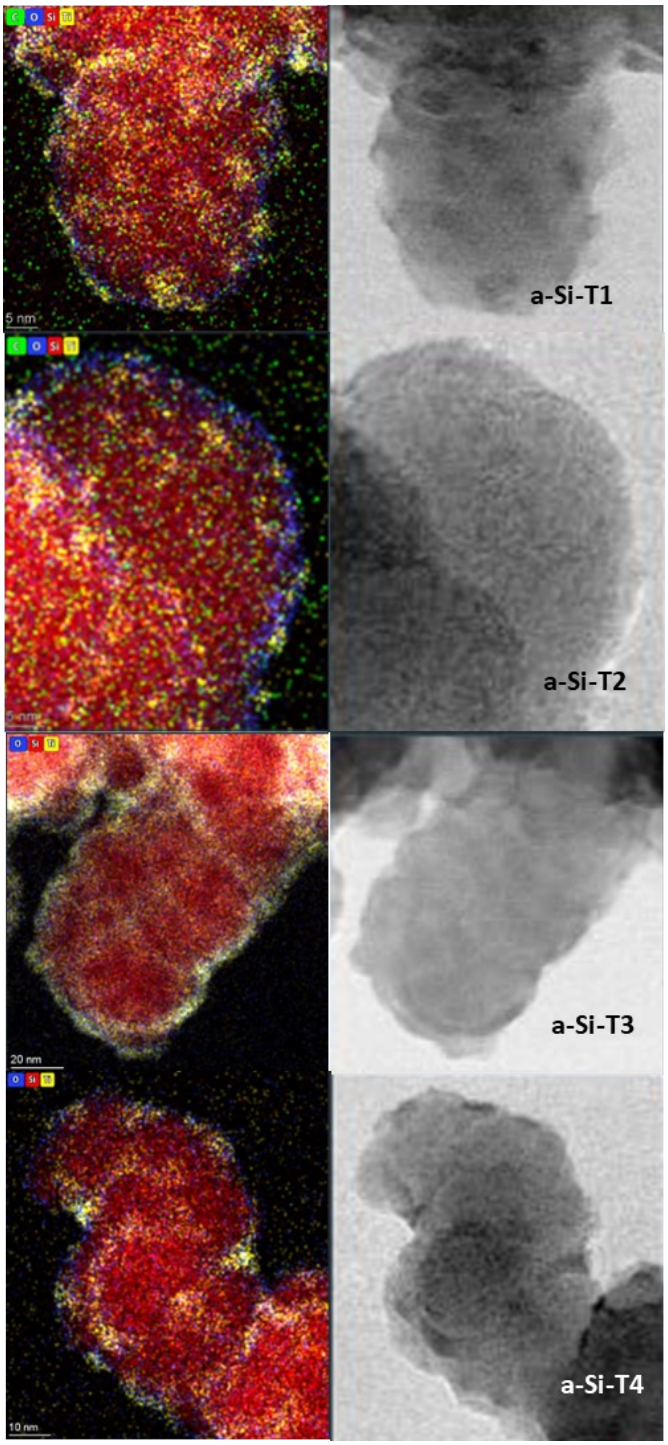

Fig. S2: EDS mapping and TEM images of TiO_2-coated silicon (a-Si-Tx, x=1-4).

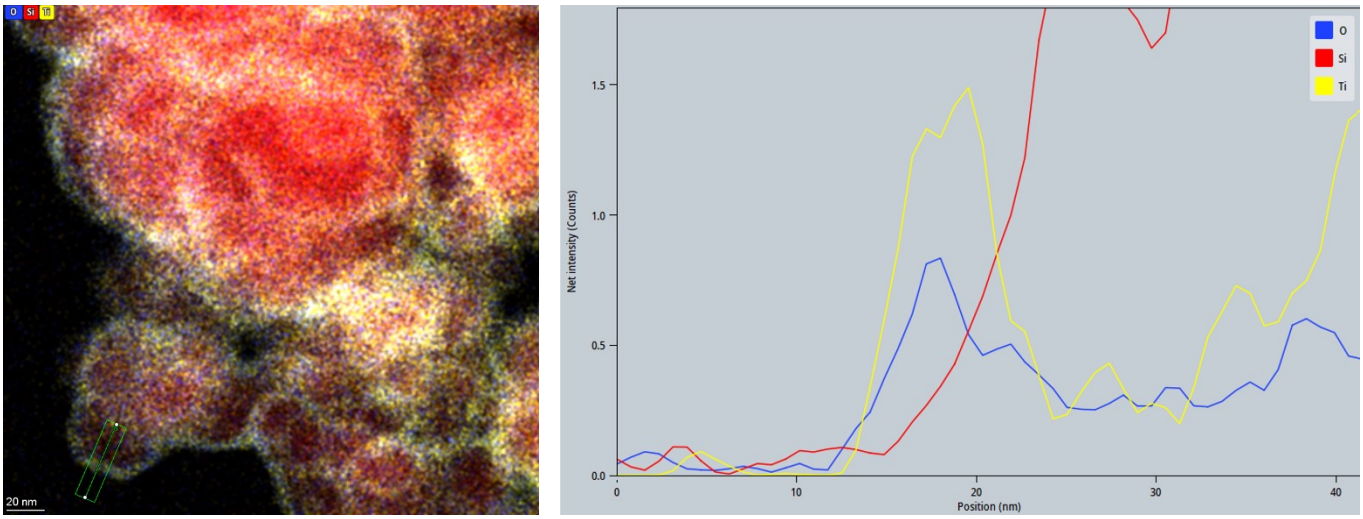

Fig. S3: EDS mapping from TEM of TiO_2-coated silicon (a-Si-T5).

X-ray photoelectron spectroscopy (XPS)

XPS analysis of battery electrodes, particularly after cycling, is challenging, due to the large number of chemically and electrically different constituents present. Differential sample charging was observed in our measurements, as is often the case.[3] This is apparent in Fig. S4, where the most electrically conducting C and Si components have different shifts in the different sample environments. Detailed identification of the specific C, O and Si components is beyond the scope of this work. Importantly, significant differences between uncoated and coated samples are not observed in the C 1s, O 1s and Si 2p spectra. Fig. S5 (left) shows Ti 2p spectra for the coated sample before cycling, which was consistent with TiO_2,[4] and after cycling, which was too weak to be analyzed. Fig. S5 (right) show Li 1s spectra of the uncoated and coated samples after cycling. Both peaks are similar and located in the region corresponding to $LiPF_6$, LiF and/or Li_2CO_3.[5] Fig. S6 shows F 1s (left) and P 2p (right) spectra for the uncoated and coated samples after cycling. The F 1s spectra show two main components where the one at highest binding energy (BE) can be assigned to $LiPF_6$ and/or $Li_xPF_yO_2$ and the one at lower BE can be assigned to LiF.[6] The P 2p spectra also show two components, assigned to $LiPF_6$ (higher BE) and $Li_xPF_yO_2$ (lower BE).[6] For both F 1s and P 2p, the relative intensity of the main components change between the uncoated and coated samples.

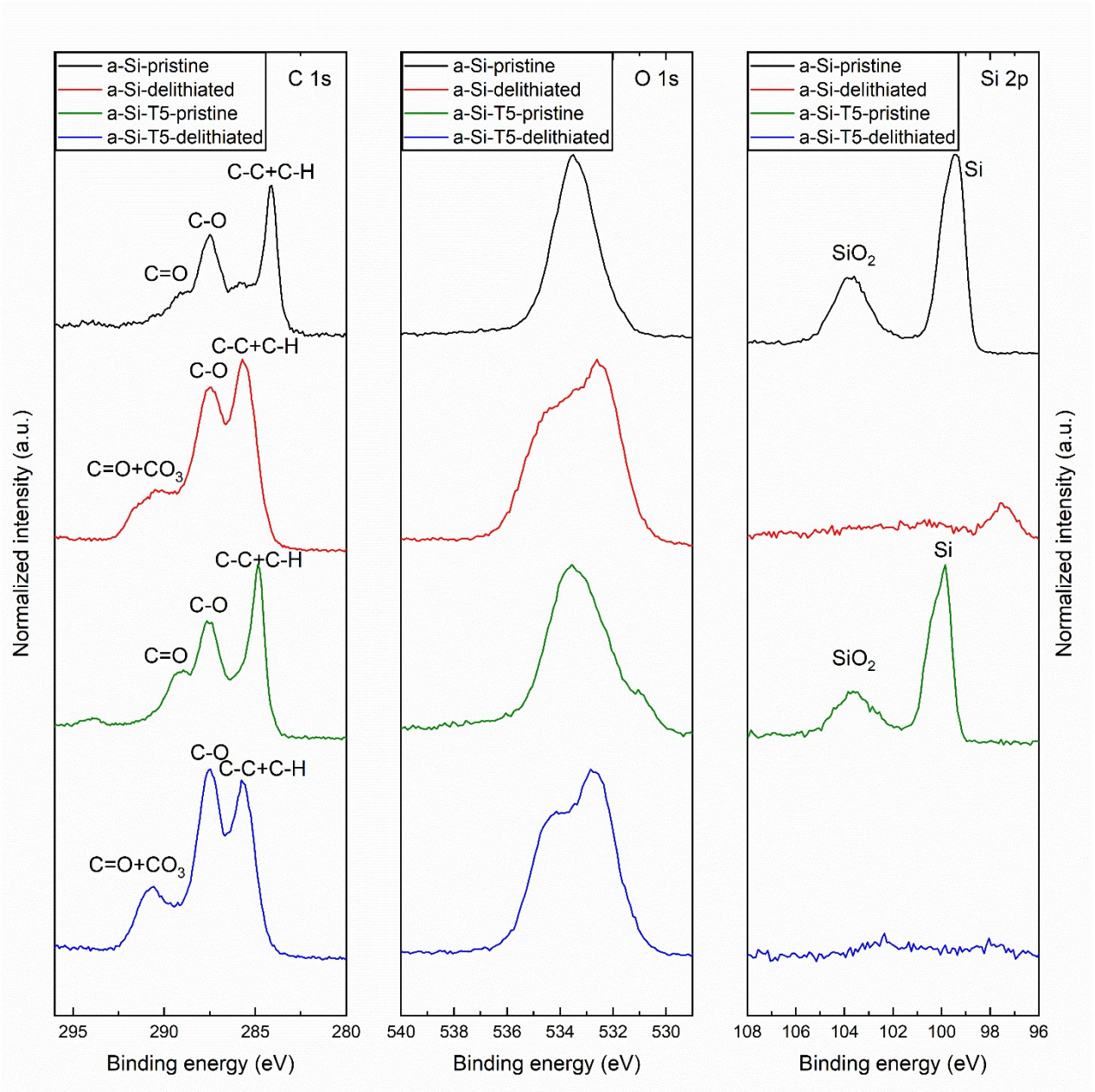

Fig. S4: High resolution XPS spectra of C 1s (left), O 1s (middle) and Si 2p (right), measured on electrodes based of uncoated amorphous silicon particles (a-Si) and TiO_2-coated silicon (a-Si-T5). The figure includes measurements of pristine electrodes and electrodes that have been extracted from coin cells after the 23rd delithiation, cycled with 1.2 M $LiPF_6$ in EC:EMC (7:3 vol%) and 2 wt% VC as electrolyte.

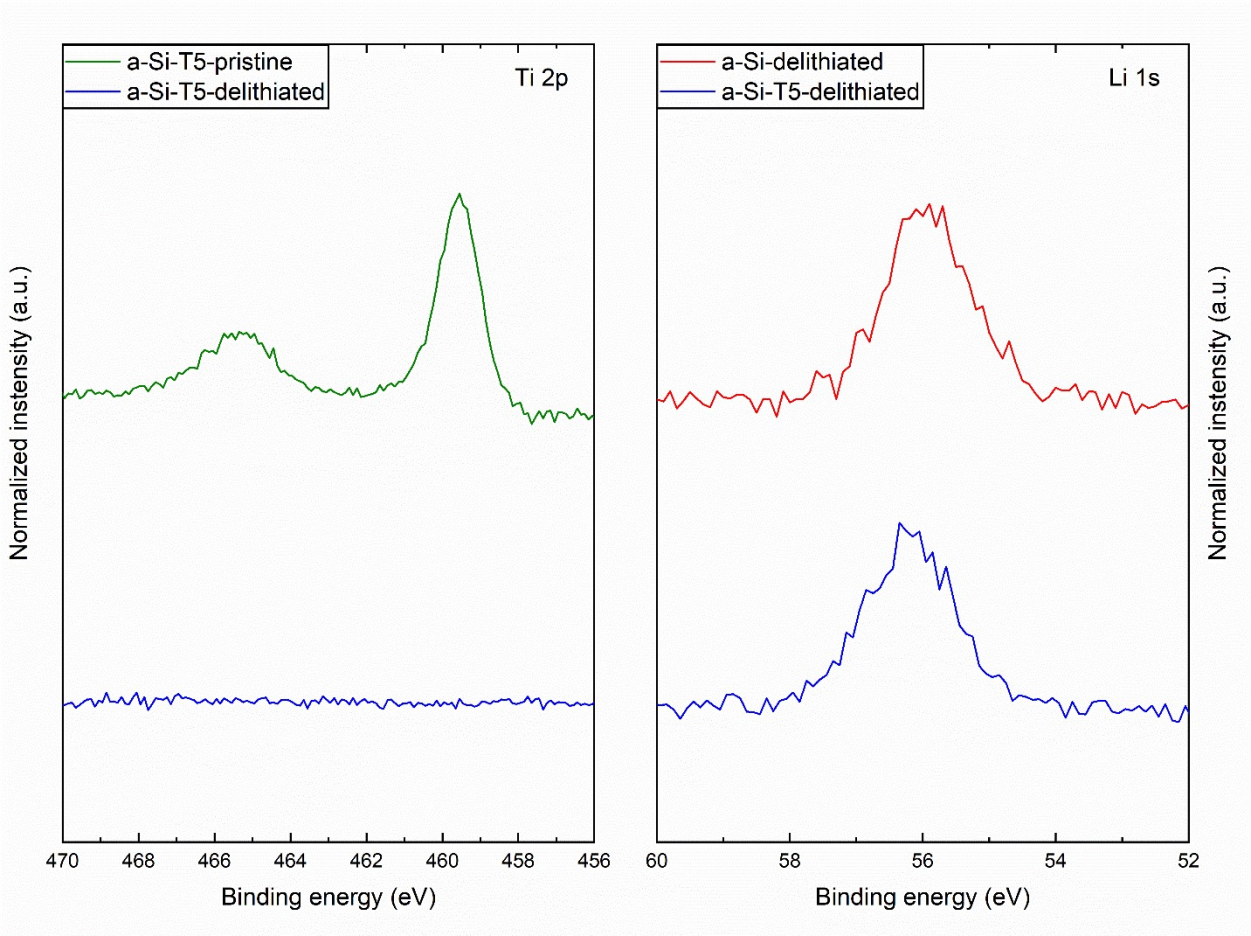

Fig. S5: High resolution XPS spectra of Ti 2p (left) and Li 1s (right), measured on electrodes based of uncoated amorphous silicon particles (a-Si) and TiO_2-coated silicon (a-Si-T5). The figure includes measurements of pristine electrodes and electrodes that have been extracted from coin cells after the 23rd delithiation, cycled with 1.2 M $LiPF_6$ in EC:EMC (7:3 vol%) and 2 wt% VC as electrolyte.

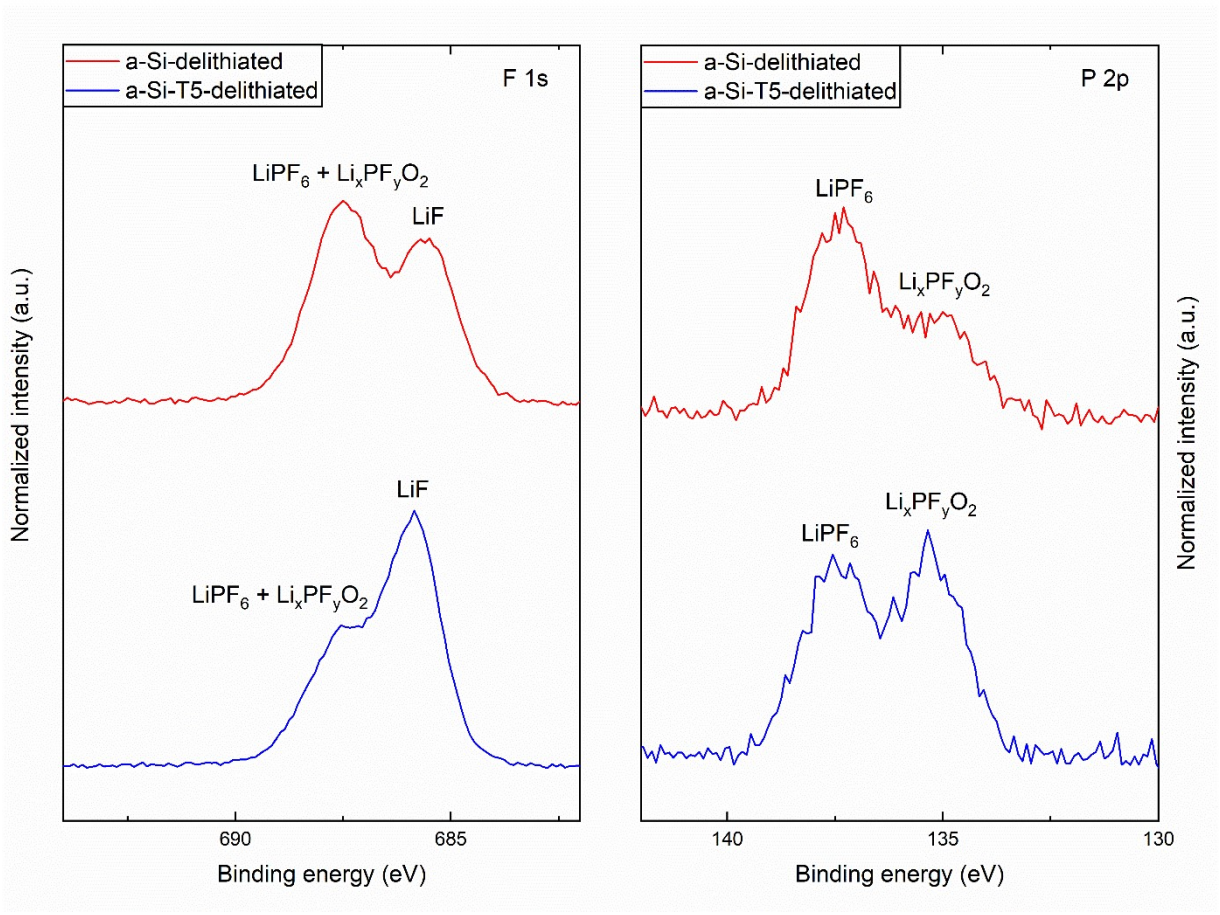

Fig. S6: High resolution XPS spectra of F 1s (left) and P 2p (right), measured on electrodes based of uncoated amorphous silicon particles (a-Si) and TiO_2-coated silicon (a-Si-T5). The figure includes measurements of pristine electrodes and electrodes that have been extracted from coin cells after the 23rd delithiation, cycled with 1.2 M $LiPF_6$ in EC:EMC (7:3 vol%) and 2 wt% VC as electrolyte.

Electrochemical characterization

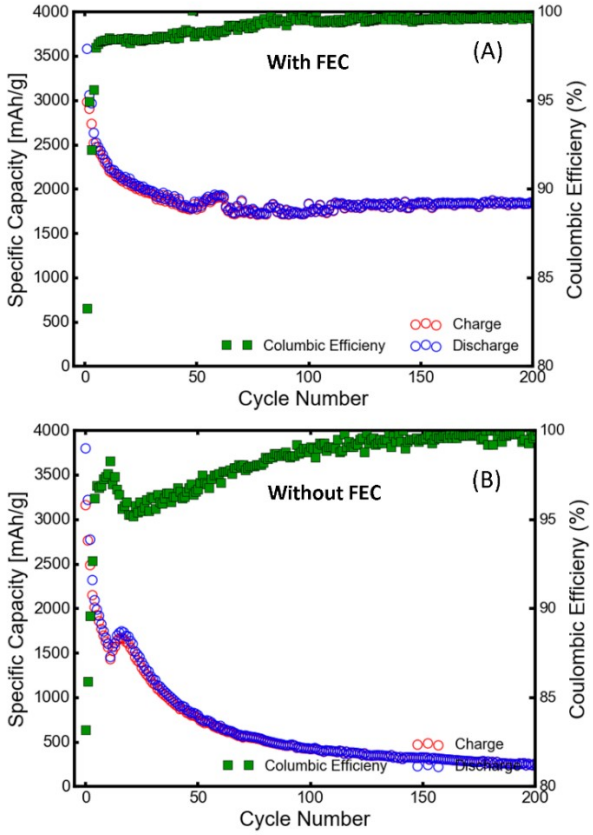

Fig. S7: Specific capacity and Coulombic efficiency extracted from galvanostatic charge-discharge cycles of pristine amorphous silicon (a-Si) with FEC (A) and without FEC (B).

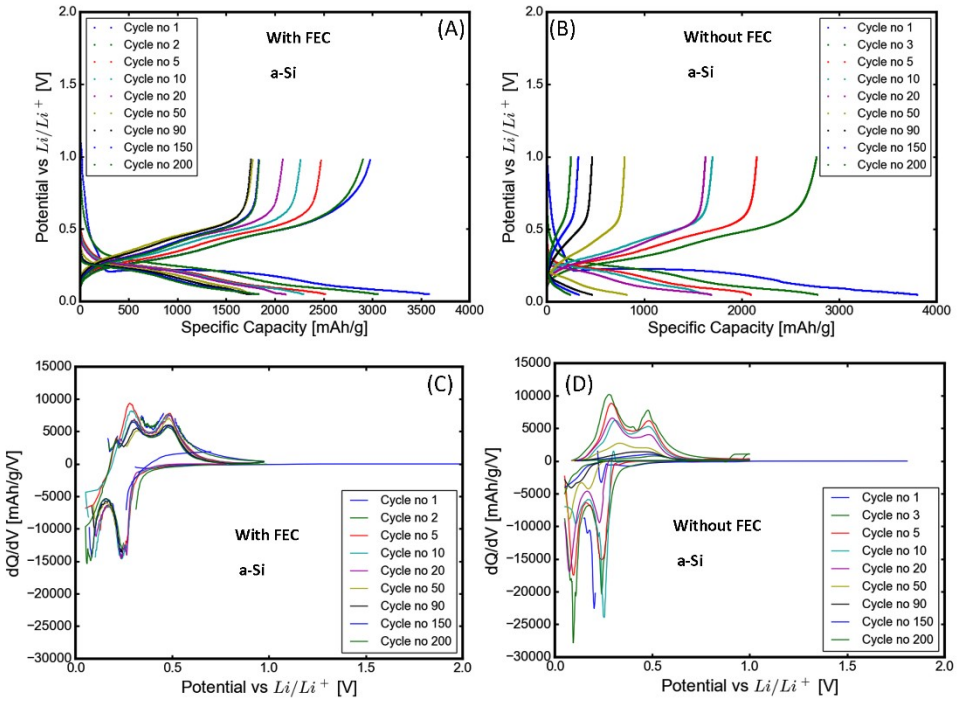

Fig. S8: Galvanostatic cycling and dQ/dV of pristine amorphous Si (a-Si) with FEC (A, C) and without FEC (B,D).

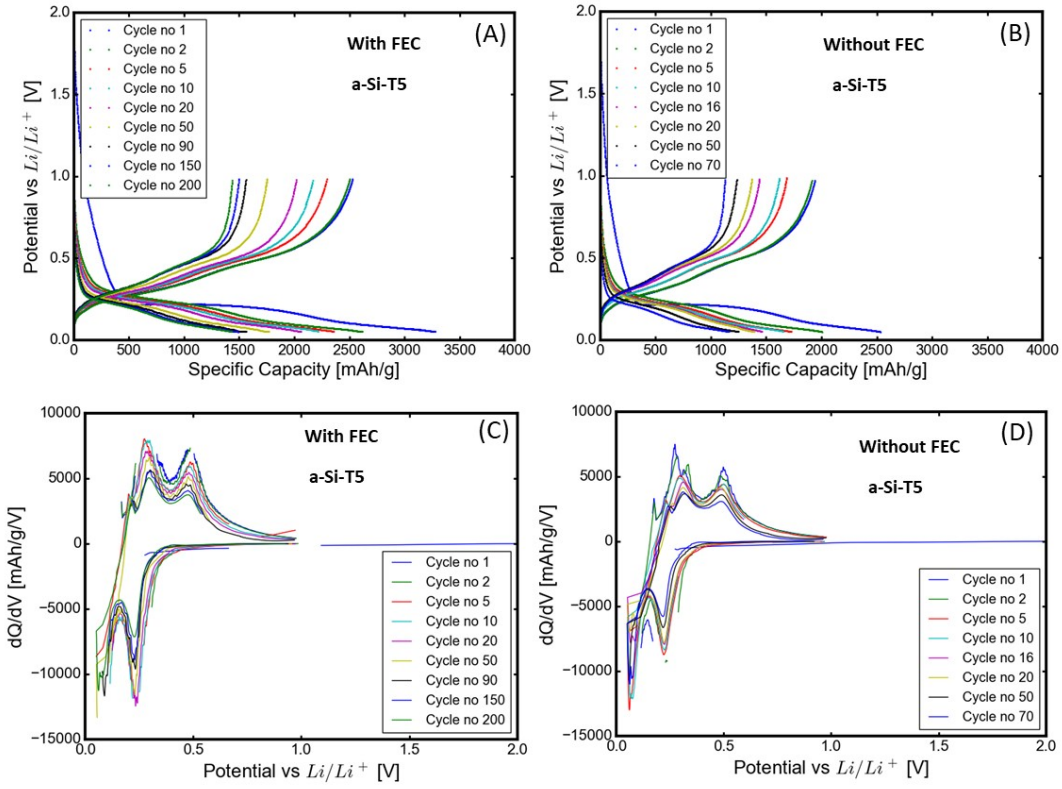

Fig. S9: Galvanostatic cycling and dQ/dV of TiO_2-coated Si (a-Si-T5) with FEC (A, C) and without FEC (B,D).

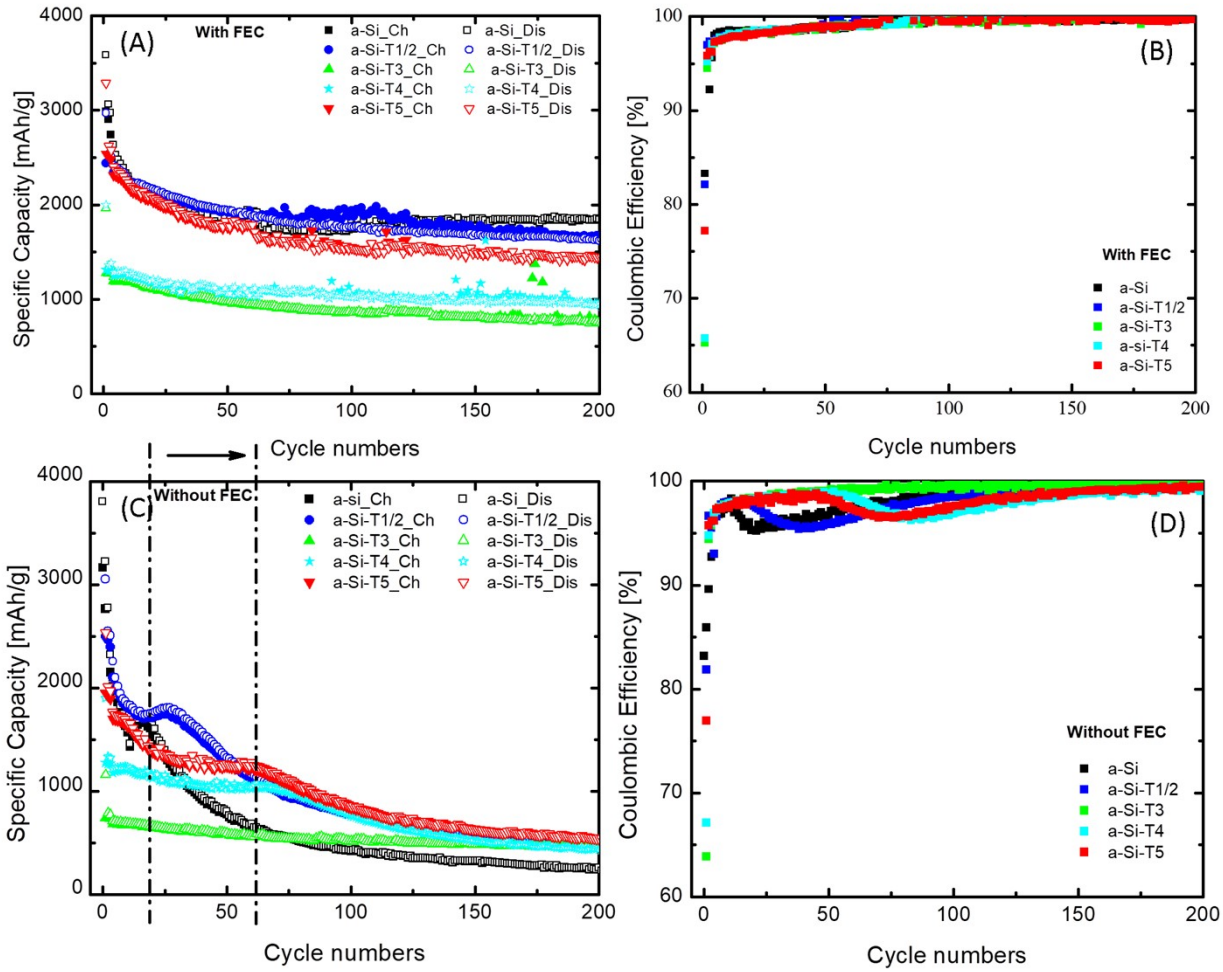

Fig. S10: Specific capacity and Coulombic efficiency of pristine and TiO_2-coated Si with FEC (A,C) and without FEC (B,D).

References

1. C. S. Ltd, CasaXPS, http://www.casaxps.com/, (accessed 12.09.2024).
2. D. A. Shirley, *Physical Review B*, 1972, **5**, 4709.
3. F. Lindgren, D. Rehnlund, I. Källquist, L. Nyholm, K. Edström, M. Hahlin and J. Maibach, *The Journal of Physical Chemistry C*, 2017, **121**, 27303-27312.
4. M. C. Biesinger, L. W. M. Lau, A. R. Gerson and R. S. C. Smart, *Applied Surface Science*, 2010, **257**, 887-898.
5. S. Leroy, F. Blanchard, R. Dedryvère, H. Martinez, B. Carré, D. Lemordant and D. Gonbeau, *Surface and Interface Analysis*, 2005, **37**, 773-781.
6. L. Gehrlein, C. Njel, F. Jeschull and J. Maibach, *ACS Applied Energy Materials*, 2022, **5**, 10710-10720.